c-Kit modifies the inflammatory status of smooth muscle cells

Lei Song [1], **Laisel Martinez** [2], **Zachary M Zigmond** [1], **Diana R Hernandez** [2], **Roberta M Lassance-Soares** [2], **Guillermo Selman** [2], **Roberto I Vazquez-Padron** [Corresp. 2]

[1] Department of Molecular and Cellular Pharmacology, University of Miami, Miami, FL, United States

[2] Department of Surgery, University of Miami, Miami, FL, United States

Corresponding Author: Roberto I Vazquez-Padron
Email address: rvazquez@med.miami.edu

Background: c-Kit is a receptor tyrosine kinase present in multiple cell types including vascular smooth muscle cells (SMC). However, little is known about how c-Kit influences SMC biology and vascular pathogenesis. **Methods:** In the present investigation, we used high-throughput microarray assays and in silico pathway analysis to elucidate the impact of c-Kit loss of function on SMC biology. We sought for differentially expressed genes between c-Kit deficient ($Kit^{W/W-v}$) and control ($Kit^{+/+}$) primary SMC. In addition, we used real-time PCR and confirmatory functional assays to further investigate the phenotypic changes detected between both types of cells by microarray analysis. **Results:** We found enhanced NF-κB gene expression and signaling secondary to the loss of c-Kit in mutant cells but not in those from littermate control mice. This included the upregulation of both the canonical and alternative NF-κB pathways. Upon stimulation with an oxidized phospholipid, deficient SMC displayed enhanced NF-κB transcriptional activity, higher phosphorylated/total p65 ratio, and increased protein expression of NF-κB regulated pro-inflammatory mediators with respect to those cells from c-Kit control mice. The pro-inflammatory phenotype of mutant cells was ameliorated after restoring c-Kit activity using lentiviral transduction. Furthermore, we demonstrated that c-Kit suppresses NF-κB activity in a TGFβ-activated kinase 1 (TAK1) and Nemo-like kinase (NLK) dependent manner. **Discussion:** In conclusion, our study suggests a novel mechanism by which c-Kit suppresses NF-κB regulated pathways in SMC, such as those leading to their pro-inflammatory transformation.

c-Kit Modifies the Inflammatory Status of Smooth Muscle Cells

Lei Song[a], Laisel Martinez[b], Zachary M. Zigmond[a], Diana R. Hernandez[b], Roberta M. Lassance-Soares[b], Guillermo Selman[b], and Roberto I. Vazquez-Padron [b,*]

[a] Molecular and Cellular Pharmacology Department, Leonard M. Miller School of Medicine, University of Miami, Miami, FL 33136

[b] DeWitt Daughtry Family Department of Surgery, Division of Vascular Surgery, Leonard M. Miller School of Medicine, University of Miami, Miami, FL 33136

Abstract word count: 232

Text word count:

[*] **Corresponding Author:**

Roberto I. Vazquez-Padron, PhD

1600 NW 10th Ave, RMSB 1048

Miami, FL 33136, United States

Tel: (305) 243-1154

Fax: (305) 243-3134

Email: RVazquez@med.miami.edu

ABSTRACT

Background: c-Kit is a receptor tyrosine kinase present in multiple cell types including vascular smooth muscle cells (SMC). However, little is known about how c-Kit influences SMC biology and vascular pathogenesis. **Methods:** In the present investigation, we used high-throughput microarray assays and in silico pathway analysis to elucidate the impact of c-Kit loss of function on SMC biology. We sought for differentially expressed genes between c-Kit deficient ($Kit^{W/W\text{-}v}$) and control ($Kit^{+/+}$) primary SMC. In addition, we used real-time PCR and confirmatory functional assays to further investigate the phenotypic changes detected between both types of cells by microarray analysis. **Results:** We found enhanced NF-κB gene expression and signaling secondary to the loss of c-Kit in mutant cells but not in those from littermate control mice. This included the upregulation of both the canonical and alternative NF-κB pathways. Upon stimulation with an oxidized phospholipid, deficient SMC displayed enhanced NF-κB transcriptional activity, higher phosphorylated/total p65 ratio, and increased protein expression of NF-κB regulated pro-inflammatory mediators with respect to those cells from c-Kit control mice. The pro-inflammatory phenotype of mutant cells was ameliorated after restoring c-Kit activity using lentiviral transduction. Furthermore, we demonstrated that c-Kit suppresses NF-κB activity in a TGFβ-activated kinase 1 (TAK1) and Nemo-like kinase (NLK) dependent manner. **Discussion:** In conclusion, our study suggests a novel mechanism by which c-Kit suppresses NF-κB regulated pathways in SMC, such as those leading to their pro-inflammatory transformation.

Keywords: c-Kit, inflammation, NF-κB, NLK, POVPC, smooth muscle cell, TAK1

Abbreviations: MCP-1, monocyte chemoattractant protein-1; MMP-2, matrix metalloproteinase-2; NF-κB, nuclear factor kappa B; NLK, Nemo-like kinase; POVPC, 1-palmitoyl-2-(5-oxovaleroyl)-*sn*-glycero-3-phosphocholine; SMC, smooth muscle cell; TAK1, transforming growth factor beta-activated kinase 1

INTRODUCTION

The c-Kit receptor tyrosine kinase is a proto-oncogene and stem cell marker that has been recently implicated in hemostasis and vascular pathogenesis. On one hand, animal models indicate that c-Kit activation by stem cell factor (SCF) plays an important role in the development of both arterial and venous intimal hyperplasia (IH) (Hollenbeck et al. 2004; Skartsis et al. 2014; Wang et al. 2006; Wang et al. 2007). SCF/c-Kit signaling is thought to suppress SMC apoptosis by inducing the Akt-Bcl-2 regulatory cascade (Wang et al. 2007). This receptor also participates in the pathological remodeling of the pulmonary vasculature through activation of the ERK1/2 pathway (Montani et al. 2011; Young et al. 2016). On the other hand, c-Kit expression preserves the SMC contractile phenotype (Davis et al. 2009) and protects arteries from excessive atherosclerosis (Song et al. 2016b). Therefore, whether c-Kit is beneficial or detrimental for the vasculature is still a matter of debate and warrants further investigations.

Interestingly, c-Kit expression in the vasculature seems to be tightly regulated by a variety of physiological and pathological triggers. Mobilization of c-Kit positive SMC toward the intima in arteries and veins has been observed after vascular injury in models of angioplasty and vein grafting (Hollenbeck et al. 2004; Wang et al. 2006; Wang et al. 2007). In addition, the contribution of c-Kit expressing adventitial progenitors and myofibroblasts to venous IH in arteriovenous fistulas occurs in response to hemodynamic changes (Skartsis et al. 2014). In the pulmonary vasculature, SCF/c-Kit signaling potentiates remodeling after hypoxic stimulation (Young et al. 2016). Paradoxically, the presence of c-Kit prevents the pathological de-differentiation of SMC *in vitro*, suggesting a protective role under certain vascular conditions (Davis et al. 2009). Contrary to previous beliefs (Wang et al. 2007), the contribution of c-Kit expressing bone marrow (BM) progenitors to vascular lesions has been shown to be minimal

(Bentzon et al. 2006), Unfortunately, there is scarce information about the molecular pathways downstream of c-Kit activation in SMC (Wang et al. 2007).

In this work, we used high-throughput microarray analyses to identify differentially expressed genes as the result of c-Kit loss of function in arterial SMC isolated from mutant and littermate control mice. We combined *in silico* pathway analyses and confirmatory assays to further investigate the phenotypic profiles of stimulated SMC under both experimental conditions. We showed increased NF-κB activation in c-Kit deficient SMC compared to their wild type counterparts. Furthermore, we demonstrated that these changes were associated with a heightened state of vascular inflammation, as indicated by the elevated protein expression of pro-inflammatory mediators in c-Kit deficient SMC. Outcomes from this study challenge the existing belief that vascular c-Kit expression is pathological and suggest instead a beneficial contribution of this signaling axis on the preservation of SMC's anti-inflammatory status under adverse conditions.

MATERIALS AND METHODS

Smooth Muscle Cell Isolation and Culture

Primary aortic SMC were isolated from c-Kit deficient ($Kit^{W/W-v}$) mice and control littermate mice ($Kit^{+/+}$) (Stock #100410, The Jackson Laboratories, Bar Harbor, ME) (Bernstein et al. 1990) using the explant technique (Metz et al. 2012) with minor modifications. Briefly, mouse aortas were digested with collagenase type II (5 mg/mL, Worthington, Lakewood, NJ) at 37°C for 1 hour, after which they were transferred to 10% FBS and cut with a scalpel into small pieces. Individual SMC migrate out of the explants within 1 week of culture. Cells were

maintained in DMEM-F12-FBS (5:3:2; Thermo Fisher Scientific, Waltham, MA) supplemented with 100 μg/ml penicillin, 100 μg/ml streptomycin, 0.1 mM glutamine, 10 mM sodium pyruvate, and 0.75% sodium bicarbonate (Metz et al. 2012). Primary cells were maintained at ~90% confluency and used within three passages to avoid fibroblast-like phenotypic switch. All animal procedures were performed according to the National Institutes of Health guidelines (Guide for the Care and Use of Laboratory Animals) and approved by the University of Miami Miller School of Medicine Institutional Animal Care and Use Committee (protocol 15-114).

RNA Microarray and Pathway Analysis

Total RNA was isolated from $Kit^{+/+}$ and $Kit^{W/W\text{-}v}$ SMC using the Quick-RNA MiniPrep kit (Zymo Research, Irvine, CA). RNA quality was validated in the Agilent 2100 Bioanalyzer (Agilent Technologies, Santa Clara, CA) before being sent to Ocean Ridge Biosciences (Palm Beach Gardens, FL) for Mouse MI-Ready Gene Expression Microarray analysis. Once in Ocean Ridge Biosciences, RNA processing included a 30-minute digestion with RNase-free DNase I (Epicentre, Madison, WI) at 37°C followed by purification using the AgenCourt RNAClean XP bead method (Beckman Coulter, Indianapolis, IN). Biotin-labeled complementary RNA (cRNA) was prepared from 2 μg per sample of re-purified RNA by the method of Van Gelder *et al*. (Van Gelder's Multi-gene expression profile - US Patent 7049102). 18 μg of biotinylated cRNA per sample were fragmented, diluted in formamide-containing hybridization buffer, and loaded onto the surface of the Mouse MI-Ready microarray slides enclosed in custom hybridization chambers. The slides were hybridized for 16-18 hours under constant rotation in a Model 400 hybridization oven (Scigene, Sunnyvale, CA). After hybridization, the microarray slides were washed under stringent conditions, stained with Streptavidin-Alexa-647 (Life Technologies,

Waltham, MA), and scanned using an Axon GenePix 4000B scanner (Molecular Devices, Sunnyvale, CA). Probe intensities were calculated for each feature on each microarray by subtracting the median local background from the median local foreground for each probe. Data for all manufacturer-flagged probes and visually flagged probes impacting >25% of samples were removed. Data for visually flagged probes impacting < 25% of samples were replaced with the sample average for the probe. Probe intensities were transformed by taking the base 2 logarithm of each value. Array-specific detection thresholds (T) were calculated by adding 3 times the standard deviation of the median local background and the mean negative control probe signal. Probe intensities and T were then normalized by subtracting the 70th percentile of the mouse probe intensities and adding back the mean of the 70th percentile across all samples as a scaling factor. The data were filtered to select for mouse probes showing signal above the normalized T in at least 25% of the samples; data for control sequences and other non-mouse probes were removed. Mouse probe sequences were annotated using a BLAST analysis of the Ensembl Mouse cDNA database version 84 (2016). Gene expression differences between $Kit^{+/+}$ and $Kit^{W/W\text{-}v}$ SMC were considered statistically significant if $p<0.05$ by *t-test*.

For pathway analysis, genes with statistically significant expression differences in microarray analysis were imported into the Ingenuity Pathway Analysis software (www.ingenuity.com; Ingenuity Systems, Redwood City, CA). The Core Analysis was used to identify the canonical pathways associated with the differentially expressed genes. Pathway overlap and p-value calculations were performed using the reference gene set in the Ingenuity Knowledge Base, where only molecular relationships (direct and indirect) that have been experimentally observed were considered. The Molecule Activity Predictor tool was used to

estimate activation or inhibition of pathway branches based on the observed gene expression fold changes in $Kit^{W/W-v}$ vs. $Kit^{+/+}$ SMC.

Quantitative Real-Time PCR (qPCR)

Relative gene expression of selected mRNA transcripts was evaluated using TaqMan Gene Expression Assays (Applied Biosystems, Foster City, CA). Total RNA was isolated as described above, and cDNA synthesized with the High-Capacity cDNA Reverse Transcription kit (Applied Biosystems). Real-time PCR was performed on an ABI Prism 7500 Fast Real-Time PCR System (96-well plate) (Applied Biosystems) using primers/probe sets complementary to the genes of interest (*ActB*, Mm00607939-m1; *Ikbka*, Mm00432529-m1; *Ikbkb*, Mm01222247-m1; *Ikbkg*, Mm00494927-m1; *Map3k14*, Mm0048444166-m1; *Nfkb2*, Mm00479807-m1; *Nfkbia*, Mm00477798-m1; *RelB*, Mm00485664-m1). Relative gene expression was determined using the ΔΔCT method (Livak & Schmittgen 2001) and normalized with respect to *ActB.*

Gene Rescue and Knockdown

Gene rescue in c-Kit deficient ($Kit^{W/W-v}$) SMC was performed using a lentiviral vector (pRVPG24). This rescue vector was constructed by inserting a blunted BsrBI-NotI digested DNA fragment (3.6 Kb), containing the coding region of the mouse Kit cDNA under the murine phosphoglycerate kinase (PGK) promoter, into the blunted EcoRV-ClaI digested pLenti CMV PuroDest vector (Addgene Inc., Cambridge, MA). Third generation lentiviral stocks were produced in HEK-293 cells co-transfected with the lentiviral vector and the packaging and envelope plasmids psPAX2 and pMD2.G (Addgene Inc.). Transfections were done with the jetPRIME transfection kit (Polyplus, New York, NY). Infected cells (100 MOI) were selected in

DMEM-F12-FBS (5:3:2; Thermo Fisher Scientific) supplemented with 100 μg/ml penicillin, 100 μg/ml streptomycin, 0.1 mM glutamine, 10 mM sodium pyruvate, 0.75% sodium bicarbonate, and 10 μg/ml puromycin (Sigma, St Louis, MO).

Knockdown of TAK1 or NLK in c-Kit wild type ($Kit^{+/+}$) SMC was performed using pooled lentiviral particles carrying different target siRNAs (Supplementary Table 1; Applied Biological Materials, Richmond, Canada). An anti-GFP siRNA was used as control. Transduced cells were puromycin-selected as described above. All gene modifications were confirmed by analytical flow cytometry or Western blot (WB).

Flow Cytometry Analysis

c-Kit surface expression was evaluated by flow cytometry in SMC stained with an anti-CD117 antibody (CD117-PE, Cat# 130-091730, Miltenyi Biotec, San Diego, CA). Analytical flow cytometry was performed on a BD FACS Canto II (BD Biosciences, San Jose, CA) using the BD FACSDiva software (Becton Dickinson, Franklin Lakes, NJ). Data were analyzed using the FlowJo software (Ashland, OR).

Western Blot and Immunoprecipitation (IP)

Whole cell protein lysates were prepared in RIPA buffer supplemented with 200 mM phenylmethylsulfonyl fluoride (PMSF), 100mM sodium orthovanadate (Santa Cruz Biotechnology, Dallas, TX), and a complete protease inhibitor cocktail (Roche Life Science, Indianapolis, IN). Lysate concentration was determined using a commercial Bradford's protein assay kit (BioRad, Hercules, CA). For WB analysis, ~50 μg of sample was loaded into a NuPAGE 4-12% Bis-Tris SDS-polyacrylamide gel (Thermo Fisher Scientific) and subsequently

transferred to a PVDF membrane (GE Healthcare, Marlborough, MA). Specific proteins were detected using antibodies against c-Kit (1:1000, Cat# sc-1494, Santa Cruz Biotechnology), MCP-1, MMP-2, TAK1 (1:500, Cat# sc-1785, sc-1839, and sc-6838, Santa Cruz Biotechnology), NLK (1:1000, Cat# ab26050, Abcam, San Francisco, CA), Src (1:500, Cat# 2108S, Cell Signaling Technology, Danvers, MA), and β-Actin (1:5000, Cat# A5316, Sigma). Bound antibodies were detected after sequentially incubating the membranes with HRP-conjugated secondary antibodies. The Amersham ECL Western Blotting Detection Reagent (GE Healthcare) or SuperSignal West Femto Maximum Sensitivity Substrate Reagent (Thermo Fisher Scientific) were used for signal detection. Images were analyzed using ImageJ Pro 5.0.

For co-IP, ~200 µg of protein lysate was incubated at 4°C for 4 hours with 1 µg of anti- c-Kit (Cat# A4502, Dako, Santa Clara, CA) or TAK1 antibodies and 20 µl of Protein A/G PLUS-Agarose microbeads (Santa Cruz Biotechnologies). Microbeads were washed with cold RIPA buffer before WB analysis for c-Kit, TAK1, or NLK as indicated above.

NF-κB Promoter Activity

Primary SMC were transfected with a commercial mix of NF-κB Luc-reporter plasmids (Qiagen, Germantown, MD) using the Axama Basic Nucleofector Primary Smooth Muscle Cells electroporation kit (Cat# VPI-1004, Lonza, Walkersville, MD). Transfected cells were incubated with POVPC (Avanti Polar Lipids, Alabaster, AL) for 24 hours in serum-free medium as previously described (Pidkovka et al. 2007) before lysis using the Passive Lysis Buffer (Promega, Madison, WI). NF-κB promoter activity was determined using the Dual-Luciferase Reporter Assay System (Cat# E1910, Promega) in a Turner Biosystems Luminometer model

Glomax 20/20 (Mountain View, CA), and normalized to the Renilla luciferase activity of the kit's internal control. Promoter activity was expressed as folds of control activity.

Enzyme-Linked Immunosorbent Assay (ELISA)

The levels of cellular NF-κB p65 and phosphorylated protein (p-p65) were measured in SMC treated with POVPC as described above. Cells were lysed using the 1X Cell Extraction Buffer PTR provided in the ELISA kit (Abcam, Cambridge, MA). The ELISA was performed using the NF-κB p65 (pS536 + Total) SimpleStep Kit (Abcam) following the manufacturer's protocol. Protein levels were measured using an endpoint reading at OD 455 nm in an Ultramark Microplate Reader (BioRad).

Statistics

Results are presented as mean ± standard deviation. A two-tailed student *t-test* was used to compare the difference between two groups, and one-way ANOVA followed by a Newman-Keuls test was applied to compare the difference among multiple groups. A p value <0.05 was considered significant.

RESULTS

Different gene expression profiles in c-Kit positive and deficient smooth muscle cells

Considering the reported contribution of the c-Kit receptor to vascular remodeling processes (Hollenbeck et al. 2004; Skartsis et al. 2014; Wang et al. 2006; Wang et al. 2007; Young et al. 2016), we investigated the gene expression profiles of SMC isolated from c-Kit

deficient ($Kit^{W/W-v}$) and control littermate ($Kit^{+/+}$) mice (n=3 per strain). Out of a total of 34,265 mouse probes queried by microarray, 18,224 yielded a detectable signal above threshold and 1,086 genes were found differentially expressed between SMC from both experimental groups ($p<0.05$) (Figure 1A-B). Specifically, 564 and 522 transcripts were significantly up- and downregulated, respectively, with the loss of c-Kit activity with respect to control SMC (Figure 1A). No statistically significant differences in expression were detected by microarray in the remaining 17,138 genes.

Table 1 presents selected differentially expressed genes in c-Kit deficient SMC that are relevant for inflammation such as *Ilf2*, *Ifna14*, and *Tnfsf9* (Chan et al. 2006; Croft 2009; Zhao et al. 2005). We also show decreased expression of the anti-inflammatory genes *Foxo1*, *Gdf6*, *Igf1*, *Igf2r*, and *Lpl* (Hisamatsu et al. 2016; Savai et al. 2014; Sukhanov et al. 2007; Ziouzenkova et al. 2003). Lipoprotein lipase (*Lpl*), for example, is 14-fold lower in c-Kit deficient cells than in those isolated from littermate controls. Additional changes in c-Kit deficient SMC are associated with a downregulation of the contractile SMC phenotype (increased *Tnfaip3* and reduced *Sirt1*) (Damrauer et al. 2010; Huang et al. 2015) and higher susceptibility to calcification (decreased *Foxo1* and *Pth1r*) (Cheng et al. 2010; Deng et al. 2015). Finally, we found significant expression differences in genes that code for cell adhesion proteins and for receptors and enzymes that regulate vasomotor responses (Table 1).

Predicted activation of NF-κB signaling in c-Kit deficient cells by pathway analysis

In silico pathway analysis was used to predict the molecular pathways affected by the loss of c-Kit in SMC. A total of 71 statistically significant pathways were identified ($p<0.05$) by the software, 42 of which with a biologically relevant function in SMC. These pathways covered cellular processes such as cell survival and apoptosis, inflammation, cell adhesion, nitric oxide

256 signaling, and lipid metabolism (Table 2). Interestingly, 10 independent molecular pathways
257 were associated with NF-κB signaling, and all of them showed either predicted activation of the
258 entire pathway (5/10; z-scores ranging from 0.258 to 1.265) or of the NF-κB branch (5/10) in c-
259 Kit deficient SMC (Table 2).

260 ***Upregulation of NF-κB pathway genes in c-Kit deficient smooth muscle cells***

261 The NF-κB pathway plays a fundamental role in SMC differentiation, inflammation, and
262 response to stress signals (Mack 2011; Mehrhof et al. 2005; Ramana et al. 2004; Zahradka et al.
263 2002). Therefore, we confirmed the upregulation of components of this pathway in c-Kit
264 deficient cells by real-time PCR (Figure 1C). We found significantly higher expression levels of
265 genes that are part of both the canonical (*Ikbka, Ikbkb, Ikbkg, Nfkbia*) and alternative (*Ikbka,*
266 *Map3k14, Nfkb2, RelB*) NF-κB signaling pathways in $Kit^{W/W\text{-}v}$ vs. $Kit^{+/+}$ SMC.

267 ***Increased activity of the canonical NF-κB pathway in stimulated c-Kit deficient cells***

268 Given that the inhibitor of the canonical NF-κB pathway (*Nfkbia*) and the negative
269 regulator *Tnfaip3* are upregulated in c-Kit deficient SMC (Table 1, Figure 1C), we turned to
270 demonstrate the relationship between c-Kit expression and functional activity of the NF-κB
271 signaling pathway. To further validate our findings, we rescued c-Kit expression in $Kit^{W/W\text{-}v}$
272 SMC by lentiviral transduction (Supplementary Figure 1).

273 POVPC-stimulated SMC with deficient c-Kit expression showed higher NF-κB
274 transcriptional activity compared to wild type and c-Kit rescued cells as determined by a dual
275 luciferase reporter assay (Figure 2A). Accordingly, a significantly higher ratio of the S536-
276 phosphorylated/total p65 factor was detected in $Kit^{W/W\text{-}v}$ SMC vs. wild type and rescued cells
277 (Figure 2B), demonstrating increased availability of active p65 in c-Kit deficient SMC for

nuclear translocation and promoter binding (Lawrence 2009). Finally, we evaluated the protein concentrations of the pro-inflammatory mediators MMP-2 and MCP-1 in POVPC-stimulated SMC, two factors that are regulated by NF-κB (Lee et al. 2008; Song et al. 2016a). In agreement with the enhanced transcriptional activity shown above, the protein expressions of both MMP-2 and MCP-1 were significantly higher in $Kit^{W/W-v}$ SMC compared to wild type and rescued cells (Figure 2C).

c-Kit regulates NF-κB activation through TAK1/NLK in smooth muscle cells

Previous studies indicate an association between c-Kit, Lyn (a member of the Src family of non-receptor tyrosine kinases), and TAK1 (Drube et al. 2015), a negative regulator of NF-κB signaling (Ajibade et al. 2012). Therefore, we assessed whether this latter factor or its downstream partner NLK (Li et al. 2014; Yasuda et al. 2004) were responsible for the observed inhibition of the NF-κB pathway in c-Kit expressing SMC. We found that the protein expressions of both TAK1 and NLK were reduced or lost in $Kit^{W/W-v}$ SMC compared to wild type or c-Kit rescued cells (Figure 3A). Next, we selectively knocked down TAK1 or NLK in $Kit^{+/+}$ SMC (Figure 3B-C**)**, and showed that this genetic manipulation restored the NF-κB transcriptional activity, phosphorylated/total p65 ratio, and protein expressions of MMP-2 and MCP1 in POVPC-stimulated c-Kit wild type SMC (Figure 3D-F). Lastly, we demonstrated by co-IP a physical interaction between all c-Kit, Src, TAK1, and NLK (Figure 4), further supporting a direct relationship in NF-κB regulation. Altogether, these experiments demonstrate that c-Kit inhibits NF-κB signaling in SMC through the actions of TAK1 and NLK.

DISCUSSION

Vascular SMC are characterized by tremendous phenotypic diversity (Yoshida & Owens 2005). Moreover, their contribution to vascular pathogenesis greatly depends on their phenotype and state of differentiation (Archer 1996; Yoshida & Owens 2005). Expression of the c-Kit receptor in SMC has been associated with various vascular pathologies in both animal models (Skartsis et al. 2014; Wang et al. 2006; Wang et al. 2007; Young et al. 2016) and human samples (Hollenbeck et al. 2004; Skartsis et al. 2014). In contrast, it has also proven protective in models of atherosclerosis (Song et al. 2016b). In light of this evidence, there is little information on how c-Kit influences the phenotypes of SMC or the mechanisms by which they contribute to pathology. Our work reveals that the absence of c-Kit modified the expression of approximately 6% of the genes that were detected by microarray in SMC from c-Kit mutant and littermate control mice. Furthermore, we provide evidence that c-Kit suppresses NF-κB signaling in SMC and decreases the production of pro-inflammatory mediators under stimulus.

Using *in silico* pathway analysis, we first demonstrated that c-Kit signaling influences a wide variety of cellular processes in SMC. Specifically, we found evidence of a pro-synthetic and pro-inflammatory phenotype in SMC secondary to the loss of this receptor. This is particularly evident by the potential dysregulation of lipid metabolism as indicated by a 14-fold decrease in *Lpl* gene expression. While increased vascular lipoprotein lipase can be pro-atherogenic (Clee et al. 2000), it is also believed to have anti-inflammatory properties both by generating metabolic PPAR agonists and inhibiting NF-κB activity (Kota et al. 2005; Ziouzenkova et al. 2003). c-Kit deficient cells also have decreased expression of the anti-inflammatory and anti-atherogenic factor IGF-1 (Sukhanov et al. 2007) and increased susceptibility to calcification due to the downregulation of the *Foxo1* and *Pth1r* genes (Cheng et

al. 2010; Deng et al. 2015). It is possible that these changes explain the increased severity of atherosclerosis in c-Kit mutant animals (Song et al. 2016b). In addition, c-Kit deficient SMC appear to respond differently to vasomotor stimuli. Their gene expression profile indicates a significantly lower expression of vasoconstrictive G-protein coupled receptors such as the angiotensin II receptor type 1B and the arginine vasopressin receptor 1A. The response to nitric oxide may be also impaired in these cells due to a lower expression of guanylate cyclase 1 soluble subunit beta. In the absence of functional experiments, it is not clear what is the biological impact of the above differences in c-Kit deficient SMC compared to their wild type counterparts. However, these observations warrant further investigations.

Interestingly, 24% of the differentially regulated pathways identified were associated with NF-κB signaling. Furthermore, both the *in silico* analysis and our experimental data demonstrated activation of this pathway in c-Kit deficient SMC with respect to those from littermate controls. NF-κB signaling is critical for the regulation of proliferation, differentiation, stress responses, and inflammatory processes in vascular SMC (Mack 2011; Mehrhof et al. 2005; Ramana et al. 2004; Zahradka et al. 2002). Whether NF-κB activation is associated with increased proliferation or apoptosis in SMC is dependent on the upstream stimuli and the type of vessel (Mehrhof et al. 2005; Ogbozor et al. 2015; Zahradka et al. 2002). A recent study demonstrated that NF-κB activation led to increased proliferation in fibroblasts, while inducing apoptosis and inflammation in SMC (Mehrhof et al. 2005). On the other hand, NF-κB was shown to be an important intracellular mediator of angiotensin II responses, leading to SMC proliferation and migration under these conditions (Zahradka et al. 2002). In terms of cell differentiation, NF-κB is known to repress myocardin activity and cause downregulation of SMC contractile genes (Tang et al. 2008). This molecular interaction has been implicated in the origin

346 of synthetic SMC under inflammatory processes such as atherosclerosis (Mack 2011).
347 Interestingly, the reduced expression of *Sirt* and increased mRNA level of *Tnfaip3* in c-Kit
348 deficient cells are independently associated with downregulation of contractile genes in SMC
349 (Damrauer et al. 2010; Huang et al. 2015). These observations are in agreement with the
350 predicted de-differentiated phenotype of c-Kit deficient SMC (Davis et al. 2009) and with the
351 reported atheroprotective role of the c-Kit receptor (Song et al. 2016b). TNFAIP3 normally
352 provides a negative regulatory loop for the NF-κB pathway, including the decreased downstream
353 production of the MCP-1 inflammatory mediator (Giordano et al. 2014; Patel et al. 2006).
354 Downregulation of the *Crebbp* transcription factor is also thought to reduce NF-κB
355 transcriptional activity (Yang et al. 2010). Nonetheless, neither higher *Tnfaip3* expression nor
356 less *Crebbp* in c-Kit deficient SMC seem to have an appreciable inhibitory effect on NF-κB
357 signaling, as demonstrated by our functional experiments and the increased protein expressions
358 of the MMP-2 and MCP-1 factors.

359 Typical stimuli for NF-κB activation include cytokines, endotoxins, lipids, and
360 mechanical stress (De Martin et al. 2000; Kumar & Boriek 2003; Maziere et al. 1996). For
361 example, the oxidized phospholipid POVPC has been previously used to induce inflammation in
362 vascular SMC (Lu et al. 2013; Pidkovka et al. 2007) and NF-κB activation (Lu et al. 2013;
363 Pegorier et al. 2006; Vladykovskaya et al. 2011). As predicted by the *in silico* analysis, c-Kit
364 deficiency in SMC led to higher levels of NF-κB transcriptional activity, phosphorylation of its
365 key subunit p65, and expression of the NF-κB regulated inflammatory mediators MMP-2 and
366 MCP-1 under POVPC challenge. Gene members of the non-canonical NF-κB pathway were also
367 upregulated in mutant SMC.

Our experiments further revealed that c-Kit reduces NF-κB mediated inflammation via a direct molecular interaction with the NF-κB negative regulators TAK1 and NLK (Ajibade et al. 2012; Li et al. 2014; Morlon et al. 2005; Yasuda et al. 2004). The physical association between c-Kit, Lyn (a member of the Src family of non-receptor tyrosine kinases), and TAK1 has been previously observed in the HEK293T cell line, where these proteins form a signalosome that interacts with IKKβ, one of the catalytic units of the IκB kinase (IKK) complex (Drube et al. 2015). Nonetheless, the inhibitory activity of TAK1 on the NF-κB signaling pathway appears to be cell-specific, since in some cells it can be activating (Ajibade et al. 2012; Israel 2010). In the inhibitory instances, TAK1 blocks the phosphorylation and inactivates IKK (Ajibade et al. 2012), which in turn is unable to phosphorylate and induce proteosomal degradation of the IκB inhibitors of the NF-κB pathway (Israel 2010; Karin 1999). When active, IκB proteins prevent the nuclear translocation of p65/RelA complexes (Israel 2010; Karin 1999). NLK also functions as an inhibitor of IKK phosphorylation (even in cells where TAK1 acts as an activator) (Li et al. 2014). Therefore, our data indicate that in SMC the roles of TAK1 and NLK may be redundant.

In conclusions, our study demonstrates that c-Kit expression in SMC has an anti-inflammatory role. Our mechanistic studies contradict the existing belief about the noxious effect of SCF/c-Kit signaling to the vasculature. It is noteworthy to recognize that such idea originated from descriptive studies and models of post injury IH. The current knowledge describes the expression of SCF and its receptor c-Kit in endothelial cells and SMC (Hollenbeck et al. 2004; Matsui et al. 2004; Skartsis et al. 2014; Wang et al. 2007), and suggests a key role for this signaling pathway in myofibroblast mobilization towards the neointima (Hollenbeck et al. 2004; Skartsis et al. 2014). Increased survival of SCF-treated SMC through Akt has also been demonstrated (Wang et al. 2007). In contrast, one recent study revealed that SCF/c-Kit signaling

protects hyperlipidemic ApoE$^{-/-}$ mice from excessive atherosclerotic plaque deposition (Song et al. 2016b). This apparent discrepancy may reflect the existing differences between IH (restenosis) and atherosclerosis in terms of etiology, natural history, culprit lesions, and progenitor cell contribution to disease progression. Therefore, our results suggests that while c-Kit positive cells have a detrimental effect on proliferative vascular lesions, their presence may prove protective in inflammatory conditions such as atherosclerosis. In addition, we propose a novel pathway for NF-κB regulation downstream of c-Kit activation. This information could be relevant in the setting of atherosclerosis disease development and complications, and may shed light on new proliferation control mechanisms to address IH after vascular injury.

Conflict of Interest

The authors declare no conflicts of interest.

Funding

The National Institutes of Health grant R01-HL-109582 to RIVP supported this study.

406 **FIGURE LEGENDS**

407 **Figure 1. Loss of c-Kit function accounts for significant gene expression differences**
408 **between c-Kit deficient and wild type smooth muscle cells (SMC). A)** Venn diagram
409 indicating the numbers of differentially upregulated genes in primary SMC isolated from c-Kit
410 deficient (blue; $Kit^{W/W-v}$) and littermate control mice (red; $Kit^{+/+}$) as determined by microarray
411 analysis. The group of genes in the interception (black area) did not show statistically significant
412 differences by *t-test* between the two strains (n=3 per group). **B)** Heat map of differentially
413 expressed genes in primary SMC from c-Kit deficient and littermate control mice. **C)** Expression
414 of NF-κB related genes in c-Kit deficient vs. control SMC as determined by real-time PCR.
415 Values are shown as fold change over expression in $Kit^{+/+}$ cells; * $p<0.05$ and ** $p<0.01$ using a
416 two-tailed *t-test* assuming unequal variance, n=3 per group.

417 **Figure 2. Loss of c-Kit function in primary smooth muscle cells (SMC) is associated with**
418 **increased NF-κB activity. A)** NF-κB transcriptional activity in c-Kit deficient ($Kit^{W/W-v}$),
419 control ($Kit^{+/+}$), and c-Kit rescued SMC (Kit^{R}) after 24-hour treatment with POVPC (50 μg/ml),
420 as determined by dual-luciferase reporter assay. Transcriptional activity is represented as the
421 mean ± standard deviation (SD) of the Firefly/Renilla luciferase ratio normalized with respect to
422 the control group ($Kit^{+/+}$) (n=3 independent experiments). **B)** Phosphorylated (pS536) protein
423 levels of the NF-κB p65 subunit in POVPC-treated c-Kit deficient, control, and c-Kit rescued
424 SMC as determined by ELISA. Values are expressed as the mean ± SD of the p-p65/total p65
425 ratio normalized with respect to the control group ($Kit^{+/+}$) (n=3 independent experiments). **C)**
426 Protein expression of the NF-κB related pro-inflammatory mediators MMP-2 and MCP-1 in
427 POVPC-treated c-Kit deficient, control, and c-Kit rescued SMC as determined by Western blot.
428 Molecular weight markers are shown on the right side of the gel. Protein expression is expressed

as the mean ± SD of the MMP-2/β-actin and MCP-1/β-actin signal ratios normalized with respect to the control group ($Kit^{+/+}$) (n=3 per cell type). * $p<0.05$ and ** $p<0.01$ using a one-way ANOVA followed by a Newman-Keuls test.

Figure 3. c-Kit inhibits NF-κB activity in smooth muscle cells (SMC) through the actions of TAK1 and NLK. A) Protein expression of the TAK1 and NLK regulatory proteins in c-Kit deficient ($Kit^{W/W-v}$), control ($Kit^{+/+}$), and c-Kit rescued SMC (Kit^{R}) as determined by Western blot. Protein expression is expressed as the mean ± standard deviation (SD) of the TAK1/β-actin and NLK/β-actin signal ratios normalized with respect to the control group ($Kit^{+/+}$) (n=3 per cell type). **B-C)** Protein expression of TAK1 **(B)** and NLK **(C)** in $Kit^{+/+}$ cells transduced with lentivirus-encoded siRNAs of the corresponding targets or GFP control. Protein expression is expressed as the mean ± SD of the TAK1/β-actin and NLK/β-actin signal ratios normalized with respect to the siGFP-treated group (n=3 independent experiments). **D)** NF-κB transcriptional activity in $Kit^{+/+}$ SMC transduced with lentivirus-encoded siRNAs complementary to TAK1, NLK, or GFP after 24-hour treatment with POVPC (50 μg/ml), as determined by dual-luciferase assay. Transcriptional activity is represented as the mean ± SD of the Firefly/Renilla luciferase ratio normalized with respect to the siGFP-treated group (n=3 independent experiments). **E)** Phosphorylated (pS536) protein levels of NF-κB p65 in POVPC-treated $Kit^{+/+}$ SMC transduced with lentivirus-encoded siRNAs as determined by ELISA. Values are expressed as the mean ± SD of the p-p65/total p65 ratio normalized with respect to the siGFP-treated group (n=3 independent experiments). **F)** Protein expression of the pro-inflammatory mediators MMP-2 and MCP-1 in POVPC-treated $Kit^{+/+}$ SMC transduced with lentivirus-encoded siRNAs as determined by Western blot. Protein expression is expressed as the mean ± SD of the MMP-2/β-actin and MCP-1/β-actin signal ratios normalized with respect to the siGFP-treated group (n=3

452 independent experiments). Molecular weight markers are shown on the right side of the gels. *
453 $p<0.05$ and ** $p<0.01$ using a one-way ANOVA followed by a Newman-Keuls test.

454 **Figure 4. c-Kit forms a molecular complex with the regulatory proteins TAK1, Src, and**
455 **NLK in smooth muscle cells (SMC). A)** Diagram illustrating the proposed molecular complex
456 between c-Kit, TAK1, Src, and NLK in SMC and their inhibitory function on NF-κB
457 transcriptional activity. **B-C)** Co-immunoprecipitation experiments in control ($Kit^{+/+}$) and c-Kit
458 deficient ($Kit^{W/W\text{-}v}$) SMC using anti-c-Kit **(B)** and anti-TAK1 antibodies **(C)** to pull down protein
459 complexes. Molecular weight markers are shown on the right side of the gels, while antibodies
460 used to detect eluted proteins are indicated on the left. IP, immunoprecipitation; IB, immunoblot.

461

462

463

464

465

466

467

468

469

470

471

REFERENCES

Ajibade AA, Wang Q, Cui J, Zou J, Xia X, Wang M, Tong Y, Hui W, Liu D, Su B, Wang HY, and Wang RF. 2012. TAK1 negatively regulates NF-kappaB and p38 MAP kinase activation in Gr-1+CD11b+ neutrophils. *Immunity* 36:43-54. 10.1016/j.immuni.2011.12.010

Archer SL. 1996. Diversity of phenotype and function of vascular smooth muscle cells. *J Lab Clin Med* 127:524-529.

Bentzon JF, Weile C, Sondergaard CS, Hindkjaer J, Kassem M, and Falk E. 2006. Smooth muscle cells in atherosclerosis originate from the local vessel wall and not circulating progenitor cells in ApoE knockout mice. *Arterioscler Thromb Vasc Biol* 26:2696-2702. 10.1161/01.ATV.0000247243.48542.9d

Bernstein A, Chabot B, Dubreuil P, Reith A, Nocka K, Majumder S, Ray P, and Besmer P. 1990. The mouse W/c-kit locus. *Ciba Found Symp* 148:158-166; discussion 166-172.

Chan A, Newman DL, Shon AM, Schneider DH, Kuldanek S, and Ober C. 2006. Variation in the type I interferon gene cluster on 9p21 influences susceptibility to asthma and atopy. *Genes Immun* 7:169-178. 10.1038/sj.gene.6364287

Cheng SL, Shao JS, Halstead LR, Distelhorst K, Sierra O, and Towler DA. 2010. Activation of vascular smooth muscle parathyroid hormone receptor inhibits Wnt/beta-catenin signaling and aortic fibrosis in diabetic arteriosclerosis. *Circ Res* 107:271-282. 10.1161/CIRCRESAHA.110.219899

Clee SM, Bissada N, Miao F, Miao L, Marais AD, Henderson HE, Steures P, McManus J, McManus B, LeBoeuf RC, Kastelein JJ, and Hayden MR. 2000. Plasma and vessel wall lipoprotein lipase have different roles in atherosclerosis. *J Lipid Res* 41:521-531.

Croft M. 2009. The role of TNF superfamily members in T-cell function and diseases. *Nat Rev Immunol* 9:271-285. 10.1038/nri2526

Damrauer SM, Peterson CR, Eva C, Studer P, and Ferran C. 2010. Partial loss of A20 (Tnfaip3) promotes resistance to abdominal aortic aneurysms through altering smooth muscle cell differentiation. *Journal of the American College of Surgeons* 211:S137.

Davis BN, Hilyard AC, Nguyen PH, Lagna G, and Hata A. 2009. Induction of microRNA-221 by platelet-derived growth factor signaling is critical for modulation of vascular smooth muscle phenotype. *J Biol Chem* 284:3728-3738. 10.1074/jbc.M808788200

De Martin R, Hoeth M, Hofer-Warbinek R, and Schmid JA. 2000. The transcription factor NF-kappa B and the regulation of vascular cell function. *Arterioscler Thromb Vasc Biol* 20:E83-88.

Deng L, Huang L, Sun Y, Heath JM, Wu H, and Chen Y. 2015. Inhibition of FOXO1/3 promotes vascular calcification. *Arterioscler Thromb Vasc Biol* 35:175-183. 10.1161/ATVBAHA.114.304786

Drube S, Weber F, Gopfert C, Loschinski R, Rothe M, Boelke F, Diamanti MA, Lohn T, Ruth J, Schutz D, Hafner N, Greten FR, Stumm R, Hartmann K, Kramer OH, Dudeck A, and Kamradt T. 2015. TAK1 and IKK2, novel mediators of SCF-induced signaling and potential targets for c-Kit-driven diseases. *Oncotarget* 6:28833-28850. 10.18632/oncotarget.5008

Giordano M, Roncagalli R, Bourdely P, Chasson L, Buferne M, Yamasaki S, Beyaert R, van Loo G, Auphan-Anezin N, Schmitt-Verhulst AM, and Verdeil G. 2014. The tumor necrosis

516 factor alpha-induced protein 3 (TNFAIP3, A20) imposes a brake on antitumor activity of
517 CD8 T cells. *Proc Natl Acad Sci U S A* 111:11115-11120. 10.1073/pnas.1406259111
518 Hisamatsu D, Ohno-Oishi M, Nakamura S, Mabuchi Y, and Naka-Kaneda H. 2016. Growth
519 differentiation factor 6 derived from mesenchymal stem/stromal cells reduces age-related
520 functional deterioration in multiple tissues. *Aging (Albany NY)* 8:1259-1275.
521 10.18632/aging.100982
522 Hollenbeck ST, Sakakibara K, Faries PL, Workhu B, Liu B, and Kent KC. 2004. Stem cell factor
523 and c-kit are expressed by and may affect vascular SMCs through an autocrine pathway.
524 *J Surg Res* 120:288-294.
525 Huang K, Yan ZQ, Zhao D, Chen SG, Gao LZ, Zhang P, Shen BR, Han HC, Qi YX, and Jiang
526 ZL. 2015. SIRT1 and FOXO Mediate Contractile Differentiation of Vascular Smooth
527 Muscle Cells under Cyclic Stretch. *Cell Physiol Biochem* 37:1817-1829.
528 10.1159/000438544
529 Israel A. 2010. The IKK complex, a central regulator of NF-kappaB activation. *Cold Spring*
530 *Harb Perspect Biol* 2:a000158. 10.1101/cshperspect.a000158
531 Karin M. 1999. How NF-kappaB is activated: the role of the IkappaB kinase (IKK) complex.
532 *Oncogene* 18:6867-6874. 10.1038/sj.onc.1203219
533 Kota RS, Ramana CV, Tenorio FA, Enelow RI, and Rutledge JC. 2005. Differential effects of
534 lipoprotein lipase on tumor necrosis factor-alpha and interferon-gamma-mediated gene
535 expression in human endothelial cells. *J Biol Chem* 280:31076-31084.
536 10.1074/jbc.M412189200
537 Kumar A, and Boriek AM. 2003. Mechanical stress activates the nuclear factor-kappaB pathway
538 in skeletal muscle fibers: a possible role in Duchenne muscular dystrophy. *FASEB J*
539 17:386-396. 10.1096/fj.02-0542com
540 Lawrence T. 2009. The nuclear factor NF-kappaB pathway in inflammation. *Cold Spring Harb*
541 *Perspect Biol* 1:a001651. 10.1101/cshperspect.a001651
542 Lee SJ, Seo KW, Yun MR, Bae SS, Lee WS, Hong KW, and Kim CD. 2008. 4-Hydroxynonenal
543 enhances MMP-2 production in vascular smooth muscle cells via mitochondrial ROS-
544 mediated activation of the Akt/NF-kappaB signaling pathways. *Free Radic Biol Med*
545 45:1487-1492. 10.1016/j.freeradbiomed.2008.08.022
546 Li SZ, Zhang HH, Liang JB, Song Y, Jin BX, Xing NN, Fan GC, Du RL, and Zhang XD. 2014.
547 Nemo-like kinase (NLK) negatively regulates NF-kappa B activity through disrupting the
548 interaction of TAK1 with IKKbeta. *Biochim Biophys Acta* 1843:1365-1372.
549 10.1016/j.bbamcr.2014.03.028
550 Livak KJ, and Schmittgen TD. 2001. Analysis of relative gene expression data using real-time
551 quantitative PCR and the 2(-Delta Delta C(T)) Method. *Methods* 25:402-408.
552 10.1006/meth.2001.1262
553 Lu Y, Zhang L, Liao X, Sangwung P, Prosdocimo DA, Zhou G, Votruba AR, Brian L, Han YJ,
554 Gao H, Wang Y, Shimizu K, Weinert-Stein K, Khrestian M, Simon DI, Freedman NJ,
555 and Jain MK. 2013. Kruppel-like factor 15 is critical for vascular inflammation. *J Clin*
556 *Invest* 123:4232-4241. 10.1172/JCI68552
557 Mack CP. 2011. Signaling mechanisms that regulate smooth muscle cell differentiation.
558 *Arterioscler Thromb Vasc Biol* 31:1495-1505. 10.1161/ATVBAHA.110.221135
559 Matsui J, Wakabayashi T, Asada M, Yoshimatsu K, and Okada M. 2004. Stem cell factor/c-kit
560 signaling promotes the survival, migration, and capillary tube formation of human

umbilical vein endothelial cells. *J Biol Chem* 279:18600-18607. 10.1074/jbc.M311643200

Maziere C, Auclair M, Djavaheri-Mergny M, Packer L, and Maziere JC. 1996. Oxidized low density lipoprotein induces activation of the transcription factor NF kappa B in fibroblasts, endothelial and smooth muscle cells. *Biochem Mol Biol Int* 39:1201-1207.

Mehrhof FB, Schmidt-Ullrich R, Dietz R, and Scheidereit C. 2005. Regulation of vascular smooth muscle cell proliferation: role of NF-kappaB revisited. *Circ Res* 96:958-964. 10.1161/01.RES.0000166924.31219.49

Metz RP, Patterson JL, and Wilson E. 2012. Vascular smooth muscle cells: isolation, culture, and characterization. *Methods Mol Biol* 843:169-176. 10.1007/978-1-61779-523-7_16

Montani D, Perros F, Gambaryan N, Girerd B, Dorfmuller P, Price LC, Huertas A, Hammad H, Lambrecht B, Simonneau G, Launay JM, Cohen-Kaminsky S, and Humbert M. 2011. C-kit-positive cells accumulate in remodeled vessels of idiopathic pulmonary arterial hypertension. *Am J Respir Crit Care Med* 184:116-123. 10.1164/rccm.201006-0905OC

Morlon A, Munnich A, and Smahi A. 2005. TAB2, TRAF6 and TAK1 are involved in NF-kappaB activation induced by the TNF-receptor, Edar and its adaptator Edaradd. *Hum Mol Genet* 14:3751-3757. 10.1093/hmg/ddi405

Ogbozor UD, Opene M, Renteria LS, McBride S, and Ibe BO. 2015. Mechanism by which nuclear factor-kappa beta (NF-kB) regulates ovine fetal pulmonary vascular smooth muscle cell proliferation. *Mol Genet Metab Rep* 4:11-18. 10.1016/j.ymgmr.2015.05.003

Patel VI, Daniel S, Longo CR, Shrikhande GV, Scali ST, Czismadia E, Groft CM, Shukri T, Motley-Dore C, Ramsey HE, Fisher MD, Grey ST, Arvelo MB, and Ferran C. 2006. A20, a modulator of smooth muscle cell proliferation and apoptosis, prevents and induces regression of neointimal hyperplasia. *FASEB J* 20:1418-1430. 10.1096/fj.05-4981com

Pegorier S, Stengel D, Durand H, Croset M, and Ninio E. 2006. Oxidized phospholipid: POVPC binds to platelet-activating-factor receptor on human macrophages. Implications in atherosclerosis. *Atherosclerosis* 188:433-443. 10.1016/j.atherosclerosis.2005.11.015

Pidkovka NA, Cherepanova OA, Yoshida T, Alexander MR, Deaton RA, Thomas JA, Leitinger N, and Owens GK. 2007. Oxidized phospholipids induce phenotypic switching of vascular smooth muscle cells in vivo and in vitro. *Circ Res* 101:792-801. 10.1161/CIRCRESAHA.107.152736

Ramana KV, Friedrich B, Srivastava S, Bhatnagar A, and Srivastava SK. 2004. Activation of nuclear factor-kappaB by hyperglycemia in vascular smooth muscle cells is regulated by aldose reductase. *Diabetes* 53:2910-2920.

Savai R, Al-Tamari HM, Sedding D, Kojonazarov B, Muecke C, Teske R, Capecchi MR, Weissmann N, Grimminger F, Seeger W, Schermuly RT, and Pullamsetti SS. 2014. Pro-proliferative and inflammatory signaling converge on FoxO1 transcription factor in pulmonary hypertension. *Nat Med* 20:1289-1300. 10.1038/nm.3695

Skartsis N, Martinez L, Duque JC, Tabbara M, Velazquez OC, Asif A, Andreopoulos F, Salman LH, and Vazquez-Padron RI. 2014. c-Kit signaling determines neointimal hyperplasia in arteriovenous fistulae. *Am J Physiol Renal Physiol* 307:F1095-1104. 10.1152/ajprenal.00292.2014

Song L, Kang C, Sun Y, Huang W, Liu W, and Qian Z. 2016a. Crocetin Inhibits Lipopolysaccharide-Induced Inflammatory Response in Human Umbilical Vein Endothelial Cells. *Cell Physiol Biochem* 40:443-452. 10.1159/000452559

606 Song L, Selman G, Santos N, Martinez L, Lassance-Soares RM, Webster K, and Vazquez-
607 Padron RI. 2016b. C-kit expression in vascular smooth muscle cells protects mice against
608 excessive atherosclerosis. *Circulation* 134:A14889.
609 Sukhanov S, Higashi Y, Shai SY, Vaughn C, Mohler J, Li Y, Song YH, Titterington J, and
610 Delafontaine P. 2007. IGF-1 reduces inflammatory responses, suppresses oxidative
611 stress, and decreases atherosclerosis progression in ApoE-deficient mice. *Arterioscler*
612 *Thromb Vasc Biol* 27:2684-2690. 10.1161/ATVBAHA.107.156257
613 Tang RH, Zheng XL, Callis TE, Stansfield WE, He J, Baldwin AS, Wang DZ, and Selzman CH.
614 2008. Myocardin inhibits cellular proliferation by inhibiting NF-kappaB(p65)-dependent
615 cell cycle progression. *Proc Natl Acad Sci U S A* 105:3362-3367.
616 10.1073/pnas.0705842105
617 Vladykovskaya E, Ozhegov E, Hoetker JD, Xie Z, Ahmed Y, Suttles J, Srivastava S, Bhatnagar
618 A, and Barski OA. 2011. Reductive metabolism increases the proinflammatory activity of
619 aldehyde phospholipids. *J Lipid Res* 52:2209-2225. 10.1194/jlr.M013854
620 Wang CH, Anderson N, Li SH, Szmitko PE, Cherng WJ, Fedak PW, Fazel S, Li RK, Yau TM,
621 Weisel RD, Stanford WL, and Verma S. 2006. Stem cell factor deficiency is
622 vasculoprotective: unraveling a new therapeutic potential of imatinib mesylate. *Circ Res*
623 99:617-625. 10.1161/01.RES.0000243210.79654.fd
624 Wang CH, Verma S, Hsieh IC, Hung A, Cheng TT, Wang SY, Liu YC, Stanford WL, Weisel
625 RD, Li RK, and Cherng WJ. 2007. Stem cell factor attenuates vascular smooth muscle
626 apoptosis and increases intimal hyperplasia after vascular injury. *Arterioscler Thromb*
627 *Vasc Biol* 27:540-547.
628 Yang J, Jiang H, Chen SS, Chen J, Xu SK, Li WQ, and Wang JC. 2010. CBP knockdown
629 inhibits angiotensin II-induced vascular smooth muscle cells proliferation through
630 downregulating NF-kB transcriptional activity. *Mol Cell Biochem* 340:55-62.
631 10.1007/s11010-010-0400-2
632 Yasuda J, Yokoo H, Yamada T, Kitabayashi I, Sekiya T, and Ichikawa H. 2004. Nemo-like
633 kinase suppresses a wide range of transcription factors, including nuclear factor-kappaB.
634 *Cancer Sci* 95:52-57.
635 Yoshida T, and Owens GK. 2005. Molecular determinants of vascular smooth muscle cell
636 diversity. *Circ Res* 96:280-291. 10.1161/01.RES.0000155951.62152.2e
637 Young KC, Torres E, Hehre D, Wu S, Suguihara C, and Hare JM. 2016. Antagonism of stem cell
638 factor/c-kit signaling attenuates neonatal chronic hypoxia-induced pulmonary vascular
639 remodeling. *Pediatr Res* 79:637-646. 10.1038/pr.2015.275
640 Zahradka P, Werner JP, Buhay S, Litchie B, Helwer G, and Thomas S. 2002. NF-kappaB
641 activation is essential for angiotensin II-dependent proliferation and migration of vascular
642 smooth muscle cells. *J Mol Cell Cardiol* 34:1609-1621.
643 Zhao G, Shi L, Qiu D, Hu H, and Kao PN. 2005. NF45/ILF2 tissue expression, promoter
644 analysis, and interleukin-2 transactivating function. *Exp Cell Res* 305:312-323.
645 10.1016/j.yexcr.2004.12.030
646 Ziouzenkova O, Perrey S, Asatryan L, Hwang J, MacNaul KL, Moller DE, Rader DJ, Sevanian
647 A, Zechner R, Hoefler G, and Plutzky J. 2003. Lipolysis of triglyceride-rich lipoproteins
648 generates PPAR ligands: evidence for an antiinflammatory role for lipoprotein lipase.
649 *Proc Natl Acad Sci U S A* 100:2730-2735. 10.1073/pnas.0538015100

650

Table 1(on next page)

Table 1. Selected list of differentially expressed genes in c-Kit deficient vs. wild type smooth muscle cells

Table 1. Selected list of differentially expressed genes in c-Kit deficient vs. wild type smooth muscle cells

Gene Symbol	Gene Product	Fold Change [a]	P-Value
Transcription Factors			
Crebbp	CREB binding protein	-1.18	0.010
Foxo1	Forkhead box O1	-2.05	0.007
Ilf2	Interleukin enhancer binding factor 2	1.38	0.034
Irf3	Interferon regulatory factor 3	-1.14	0.029
Nfatc1	Nuclear factor of activated T-cells 1	-1.36	0.040
Nfatc2	Nuclear factor of activated T-cells 2	2.01	0.033
Nfatc4	Nuclear factor of activated T-cells 4	-2.32	0.009
Cell Adhesion Proteins			
Cdh5	Cadherin 5	-5.00	0.043
Itga9	Integrin subunit alpha 9	-2.91	0.047
Itga11	Integrin subunit alpha 11	-13.28	0.034
Pcdh7	Protocadherin 7	-2.71	0.015
Pcdha1	Protocadherin alpha 1	-1.44	0.042
Pcdha8	Protocadherin alpha 8	2.26	0.002
Selplg	P-selectin glycoprotein ligand 1	-3.94	0.006
Cytokines/Growth Factors			
Ccl6	Chemokine (C-C motif) ligand 6	-8.76	0.005
Gdf6	Growth differentiation factor 6	-4.10	0.019
Ifna14	Interferon alpha 14	1.27	0.043
Igf1	Insulin-like growth factor 1	-5.06	0.027
Pdgfb	Platelet-derived growth factor subunit B	-2.59	0.011
Pgf	Placental growth factor	-4.96	0.037
Tnfsf9	Tumor necrosis factor ligand superfamily member 9	2.97	0.048
Enzymes			
Bmp1	Bone morphogenetic protein 1	-2.36	0.016
Casp3	Caspase 3	2.06	0.040
Ccnd1	Cyclin D1	2.20	0.043
Gucy1b3	Guanylate cyclase 1 soluble subunit beta	-8.95	0.033
Ikbkb	Inhibitor of nuclear factor kappa-B kinase subunit beta	1.34	0.001
Lpl	Lipoprotein lipase	-14.24	0.022
Mmp23	Matrix metallopeptidase 23	-6.61	0.049
Pde1a	Ca2+/calmodulin dependent phosphodiesterase 1A	-4.73	0.028
Pde2a	Phosphodiesterase 2A	-1.91	0.048
Sirt1	Sirtuin 1	-1.52	0.034
Tnfaip3	TNF alpha induced protein 3	3.46	<0.001
Receptors			
Adra2a	Adrenoceptor alpha 2A	-6.49	0.002
Agtr1b	Angiotensin II type 1b receptor	-9.88	0.043
Avpr1a	Arginine vasopressin receptor 1A	-6.62	0.010
Cxcr4	Chemokine (C-X-C motif) receptor 4	-6.55	0.040
Igf2r	Insulin like growth factor 2 receptor	-1.48	0.012
Il3ra	Interleukin 3 receptor subunit alpha	-2.38	0.023
Il20ra	Interleukin 20 receptor alpha	-3.52	0.003
Pdgfrb	Platelet-derived growth factor receptor beta	-2.89	0.016
Pth1r	Parathyroid hormone 1 receptor	-5.42	0.002

[a] *Average fold gene expression change in c-Kit deficient smooth muscle cells compared to wild type cells.*

1

Table 2(on next page)

Table 2. Selected canonical pathways with differentially expressed genes in c-Kit deficient vs. wild type smooth muscle cells

Table 2. Selected canonical pathways with differentially expressed genes in c-Kit deficient vs. wild type smooth muscle cells

Pathway	Biological Function	P-Value	Z-Score[a]	Predicted Status[a]	Differentially Expressed Genes
PTEN signaling[b]	Proliferation, apoptosis, de-differentiation, cell migration, inflammation	<0.001	0.258	Activation	Akt2, Casp3, Rac1, Ccnd1, Igf2r, Rac3, Ddr1, Shc1, Ikbkb, Inpp5f, Foxo1, Bmpr1a, Magi2, Magi3, Pdgfrb
Death receptor signaling[b]	Apoptosis	0.003	1.265	Activation	Map2k4, Gas2, Rock1, Diablo, Ikbkb, Casp3, Htra2, Tbk1, Parp1, Birc2
TNFR2 signaling[b]	Cell survival, inflammation	0.005	1.000	Activation	Map2k4, Ikbkb, Tnfaip3, Tbk1, Birc2
Wnt/β-catenin signaling	Proliferation, cell survival, cell migration	0.008	0.577	Activation	Sfrp4, Akt2, Crebbp, Csnk1a1, Fzd9, Ccnd1, Rarg, Fzd8, Cdh5, Dkk3, Sox18, Ppp2r5e, Sfrp1, Wnt5b
IRF activation pathway[b]	Inflammation	0.011	1.134	Activation	Map2k4, Ikbkb, Crebbp, Tbk1, Ifna14, Irf3, Atf2
ERK/MAPK signaling	Proliferation, cell migration, vasoconstriction	0.028	1.069	Activation	Crebbp, Rac1, Ppp1r14a, Mknk2, Rac3, Nfatc1, Atf2, Pla2g4e, Shc1, Pla2g6, Prkar2b, Prkag2, Rps6ka1, Ppp2r5e
TNFR1 signaling[b]	Cell survival, inflammation	0.044	1.000	Activation	Map2k4, Ikbkb, Casp3, Tnfaip3, Birc2
Wnt/Ca^{2+} pathway[b]	Proliferation, cell migration	<0.001	-1.000	Inhibition	Fzd8, Plcb4, Crebbp, Nfatc2, Fzd9, Nfatc4, Wnt5b, Nfatc1, Atf2
AMPK signaling[b]	Cellular senescence, anti-inflammatory, differentiation, vasoconstriction	<0.001	-0.535	Inhibition	Pbrm1, Akt2, Crebbp, Ccnd1, Slc2a4, Elavl1, Atf2, Ak6, Prkar2b, Foxo1, Adra2a, Ppm1b, Sirt1, Prkag2, Ppm1a, Ppp2r5e, Ppat, Camkk2
Apoptosis signaling[b]	Apoptosis	<0.001	-0.302	Inhibition	Map2k4, Gas2, Rock1, Diablo, Ikbkb, Casp3, Htra2, Rps6ka1, Bcl2a1, Parp1, Birc2
Phospholipase C signaling	Vasoconstriction, stress responses	0.001	-0.378	Inhibition	Rala, Arhgef12, Pld3, Fcgr2a, Arhgef15, Crebbp, Rac1, Ppp1r14a, Nfatc4, Fcgr2b, Rhoh, Nfatc1, Atf2, Pla2g6, Shc1, Pla2g4e, Plcb4, Itpr3, Fcer1g, Nfatc2
Nitric oxide/GC signaling	Vasodilation	0.005	-0.302	Inhibition	Bdkrb2, Kng1, Pde2a, Akt2, Prkg1, Prkar2b, Itpr3, Prkag2, Pde1a, Gucy1b3, Pgf
Integrin signaling	Cell adhesion, cell migration, proliferation, apoptosis, stress responses, differentiation	0.029	-1.387	Inhibition	Map2k4, Akt2, Rala, Rac1, Rac3, Rhoh, Pdgfb, Rock1, Arhgap5, Shc1, Itga11, Itga9, Actn4, Tspan6, Nedd9
Adipogenesis pathway	Lipid synthesis and storage	<0.001	N.D.	Could not be predicted	Nr2f2, Sin3b, Fzd9, Nfatc4, Rbp1, Slc2a4, Fzd8, Cdk5, Foxo1, Bmpr1a, Lpl, Sirt1, Ctbp2, Clock, Fabp4, Rps6ka1, Stat5b
Fibroblast inflammatory pathway[b]	Proliferation, cell migration, differentiation, inflammation	0.012	N.D.	Could not be predicted	Map2k4, Sfrp4, Akt2, Crebbp, Csnk1a1, Rac1, Fzd9, Nfatc4, Ccnd1, Nfatc1, Pdgfb, Pgf, Atf2, Rock1, Ikbkb, Fzd8, Plcb4, Dkk3, Nfatc2, Sfrp1, Wnt5b
Gαq signaling[b]	Proliferation, cell migration, vasoconstriction	0.026	0.000	Could not be predicted	Rock1, Ikbkb, Plcb4, Akt2, Pld3, Agtr1b, Itpr3, Nfatc2, Nfatc4, Avpr1a, Rhoh, Nfatc1

[a] Z-score and predicted functional status in c-Kit deficient smooth muscle cells compared to wild type cells. The z-score measures how well the gene expression data matches the experimentally observed direction of pathway regulation in the literature. A positive z-score predicts activation, while a negative z-score indicates inhibition. N.D., could not be determined.

[b] NF-κB associated signaling pathway

1

Figure 1

Figure 1. Loss of c-Kit function accounts for significant gene expression differences between c-Kit deficient and wild type smooth muscle cells (SMC).

Figure 1. Loss of c-Kit function accounts for significant gene expression differences between c-Kit deficient and wild type smooth muscle cells (SMC). A) Venn diagram indicating the numbers of differentially upregulated genes in primary SMC isolated from c-Kit deficient (blue; $Kit^{W/W-v}$) and littermate control mice (red; $Kit^{+/+}$) as determined by microarray analysis. The group of genes in the interception (black area) did not show statistically significant differences by *t-test* between the two strains (n=3 per group). **B)** Heat map of differentially expressed genes in primary SMC from c-Kit deficient and littermate control mice. **C)** Expression of NF-κB related genes in c-Kit deficient vs. control SMC as determined by real-time PCR. Values are shown as fold change over expression in $Kit^{+/+}$ cells; * $p<0.05$ and ** $p<0.01$ using a two-tailed *t-test* assuming unequal variance, n=3 per group.

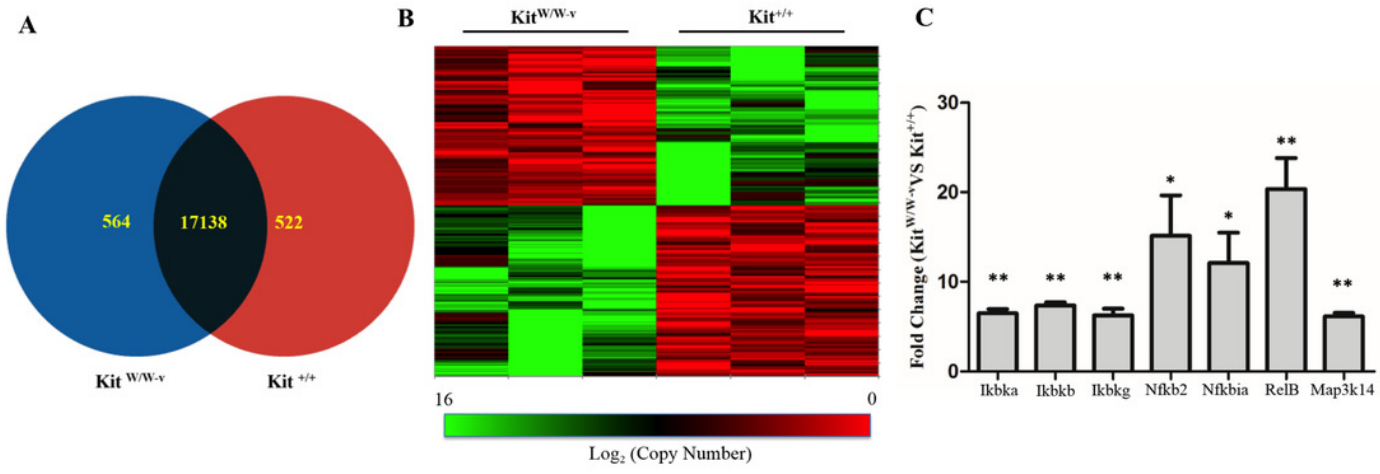

Figure 1. Loss of c-Kit function accounts for significant gene expression differences between c-Kit deficient and wild type smooth muscle cells (SMC). A) Venn diagram indicating the numbers of differentially upregulated genes in primary SMC isolated from c-Kit deficient (blue; $Kit^{W/W-v}$) and littermate control mice (red; $Kit^{+/+}$) as determined by microarray analysis. The group of genes in the interception (black area) did not show statistically significant differences by *t-test* between the two strains (n=3 per group). **B)** Heat map of differentially expressed genes in primary SMC from c-Kit deficient and littermate control mice. **C)** Expression of NF-κB related genes in c-Kit deficient vs. control SMC as determined by real-time PCR. Values are shown as fold change over expression in $Kit^{+/+}$ cells; * $p<0.05$ and ** $p<0.01$ using a two-tailed *t-test* assuming unequal variance, n=3 per group.

Figure 2

Figure 2. Loss of c-Kit function in primary smooth muscle cells (SMC) is associated with increased NF-κB activity.

Figure 2. Loss of c-Kit function in primary smooth muscle cells (SMC) is associated with increased NF-κB activity. A) NF-κB transcriptional activity in c-Kit deficient ($Kit^{W/W-v}$), control ($Kit^{+/+}$), and c-Kit rescued SMC (Kit^{R}) after 24-hour treatment with POVPC (50 µg/ml), as determined by dual-luciferase reporter assay. Transcriptional activity is represented as the mean ± standard deviation (SD) of the Firefly/Renilla luciferase ratio normalized with respect to the control group ($Kit^{+/+}$) (n=3 independent experiments). **B)** Phosphorylated (pS536) protein levels of the NF-κB p65 subunit in POVPC-treated c-Kit deficient, control, and c-Kit rescued SMC as determined by ELISA. Values are expressed as the mean ± SD of the p-p65/total p65 ratio normalized with respect to the control group ($Kit^{+/+}$) (n=3 independent experiments). **C)** Protein expression of the NF-κB related pro-inflammatory mediators MMP-2 and MCP-1 in POVPC-treated c-Kit deficient, control, and c-Kit rescued SMC as determined by Western blot. Molecular weight markers are shown on the right side of the gel. Protein expression is expressed as the mean ± SD of the MMP-2/β-actin and MCP-1/β-actin signal ratios normalized with respect to the control group ($Kit^{+/+}$) (n=3 per cell type). * $p<0.05$ and ** $p<0.01$ using a one-way ANOVA followed by a Newman-Keuls test.

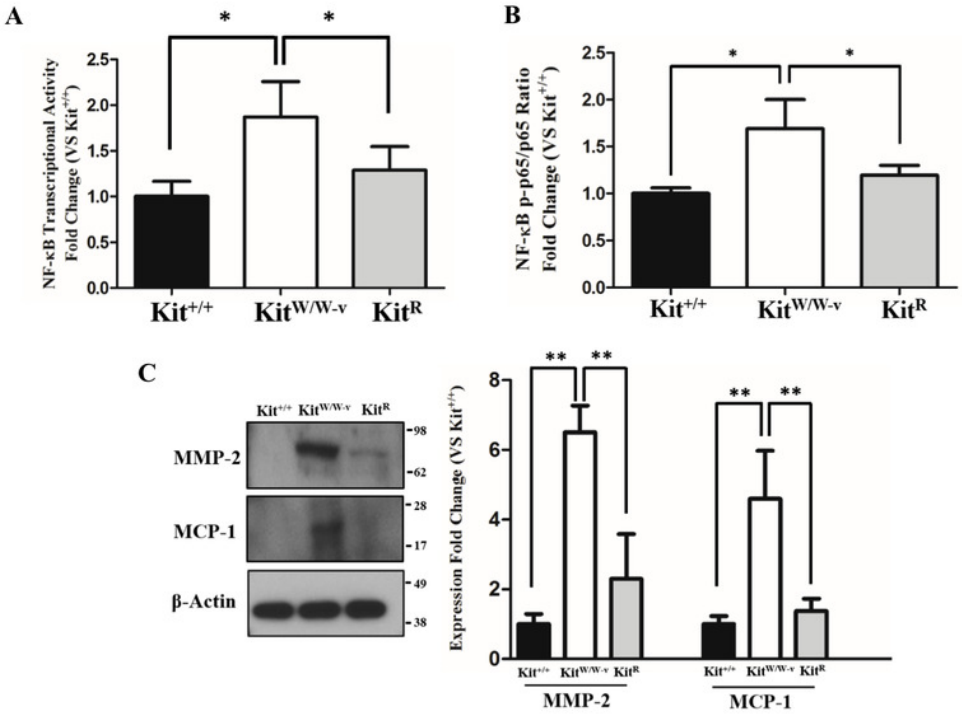

Figure 2. Loss of c-Kit function in primary smooth muscle cells (SMC) is associated with increased NF-κB activity. A) NF-κB transcriptional activity in c-Kit deficient ($Kit^{W/W-v}$), control ($Kit^{+/+}$), and c-Kit rescued SMC (Kit^{R}) after 24-hour treatment with POVPC (50 μg/ml), as determined by dual-luciferase reporter assay. Transcriptional activity is represented as the mean ± standard deviation (SD) of the Firefly/Renilla luciferase ratio normalized with respect to the control group ($Kit^{+/+}$) (n=3 independent experiments). **B)** Phosphorylated (pS536) protein levels of the NF-κB p65 subunit in POVPC-treated c-Kit deficient, control, and c-Kit rescued SMC as determined by ELISA. Values are expressed as the mean ± SD of the p-p65/total p65 ratio normalized with respect to the control group ($Kit^{+/+}$) (n=3 independent experiments). **C)** Protein expression of the NF-κB related pro-inflammatory mediators MMP-2 and MCP-1 in POVPC-treated c-Kit deficient, control, and c-Kit rescued SMC as determined by Western blot. Molecular weight markers are shown on the right side of the gel. Protein expression is expressed as the mean ± SD of the MMP-2/β-actin and MCP-1/β-actin signal ratios normalized with respect to the control group ($Kit^{+/+}$) (n=3 per cell type). * $p<0.05$ and ** $p<0.01$ using a one-way ANOVA followed by a Newman-Keuls test.

Figure 3

Figure 3. c-Kit inhibits NF-κB activity in smooth muscle cells (SMC) through the actions of TAK1 and NLK.

Figure 3. c-Kit inhibits NF-κB activity in smooth muscle cells (SMC) through the actions of TAK1 and NLK. A) Protein expression of the TAK1 and NLK regulatory proteins in c-Kit deficient ($Kit^{W/W-v}$), control ($Kit^{+/+}$), and c-Kit rescued SMC (Kit^{R}) as determined by Western blot. Protein expression is expressed as the mean ± standard deviation (SD) of the TAK1/β-actin and NLK/β-actin signal ratios normalized with respect to the control group ($Kit^{+/+}$) (n=3 per cell type). **B-C)** Protein expression of TAK1 **(B)** and NLK **(C)** in $Kit^{+/+}$ cells transduced with lentivirus-encoded siRNAs of the corresponding targets or GFP control. Protein expression is expressed as the mean ± SD of the TAK1/β-actin and NLK/β-actin signal ratios normalized with respect to the siGFP-treated group (n=3 independent experiments). **D)** NF-κB transcriptional activity in $Kit^{+/+}$ SMC transduced with lentivirus-encoded siRNAs complementary to TAK1, NLK, or GFP after 24-hour treatment with POVPC (50 μg/ml), as determined by dual-luciferase assay. Transcriptional activity is represented as the mean ± SD of the Firefly/Renilla luciferase ratio normalized with respect to the siGFP-treated group (n=3 independent experiments). **E)** Phosphorylated (pS536) protein levels of NF-κB p65 in POVPC-treated $Kit^{+/+}$ SMC transduced with lentivirus-encoded siRNAs as determined by ELISA. Values are expressed as the mean ± SD of the p-p65/total p65 ratio normalized with respect to the siGFP-treated group (n=3 independent experiments). **F)** Protein expression of the pro-inflammatory mediators MMP-2 and MCP-1 in POVPC-treated $Kit^{+/+}$ SMC transduced with lentivirus-encoded siRNAs as determined by Western blot. Protein expression is expressed as the mean ± SD of the MMP-2/β-actin and MCP-1/β-actin signal ratios normalized with respect to the siGFP-treated group (n=3 independent experiments). Molecular weight markers are shown on the right side of the gels. * $p<0.05$ and ** $p<0.01$ using a one-way ANOVA followed by a Newman-Keuls test.

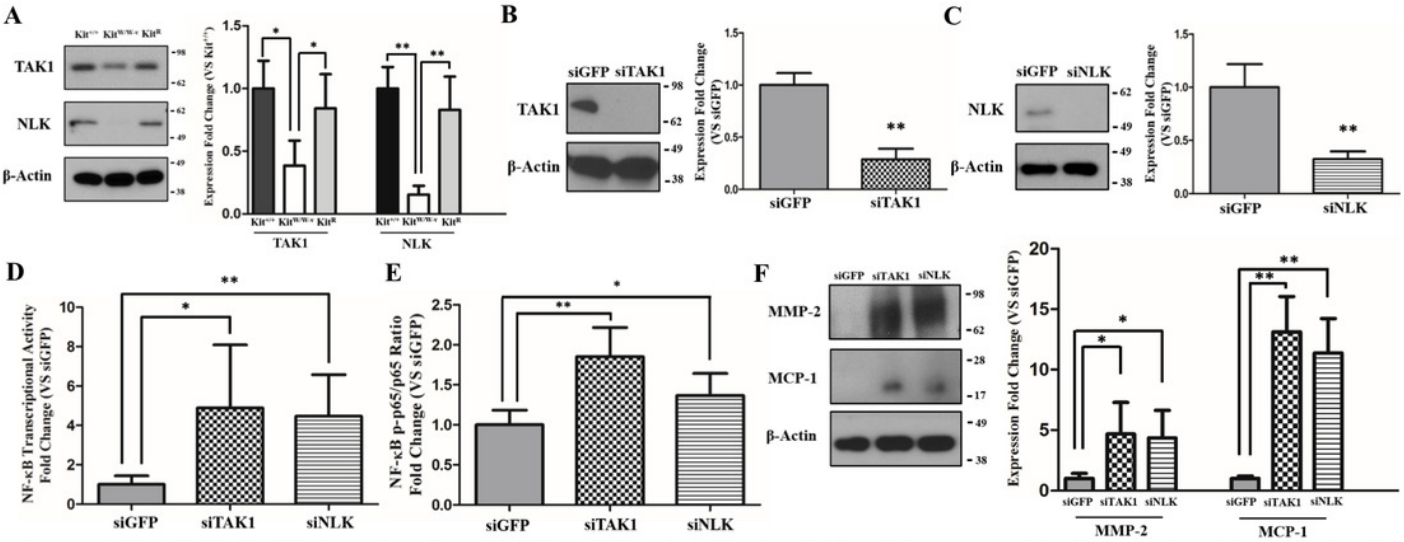

Figure 3. c-Kit inhibits NF-κB activity in smooth muscle cells (SMC) through the actions of TAK1 and NLK. A) Protein expression of the TAK1 and NLK regulatory proteins in c-Kit deficient ($Kit^{W/W-v}$), control ($Kit^{+/+}$), and c-Kit rescued SMC (Kit^{R}) as determined by Western blot. Protein expression is expressed as the mean ± standard deviation (SD) of the TAK1/β-actin and NLK/β-actin signal ratios normalized with respect to the control group ($Kit^{+/+}$) (n=3 per cell type). **B-C)** Protein expression of TAK1 **(B)** and NLK **(C)** in $Kit^{+/+}$ cells transduced with lentivirus-encoded siRNAs of the corresponding targets or GFP control. Protein expression is expressed as the mean ± SD of the TAK1/β-actin and NLK/β-actin signal ratios normalized with respect to the siGFP-treated group (n=3 independent experiments). **D)** NF-κB transcriptional activity in $Kit^{+/+}$ SMC transduced with lentivirus-encoded siRNAs complementary to TAK1, NLK, or GFP after 24-hour treatment with POVPC (50 μg/ml), as determined by dual-luciferase assay. Transcriptional activity is represented as the mean ± SD of the Firefly/Renilla luciferase ratio normalized with respect to the siGFP-treated group (n=3 independent experiments). **E)** Phosphorylated (pS536) protein levels of NF-κB p65 in POVPC-treated $Kit^{+/+}$ SMC transduced with lentivirus-encoded siRNAs as determined by ELISA. Values are expressed as the mean ± SD of the p-p65/total p65 ratio normalized with respect to the siGFP-treated group (n=3 independent experiments). **F)** Protein expression of the pro-inflammatory mediators MMP-2 and MCP-1 in POVPC-treated $Kit^{+/+}$ SMC transduced with lentivirus-encoded siRNAs as determined by Western blot. Protein expression is expressed as the mean ± SD of the MMP-2/β-actin and MCP-1/β-actin signal ratios normalized with respect to the siGFP-treated group (n=3 independent experiments). Molecular weight markers are shown on the right side of the gels. * $p<0.05$ and ** $p<0.01$ using a one-way ANOVA followed by a Newman-Keuls test.

Figure 4

Figure 4. c-Kit forms a molecular complex with the regulatory proteins TAK1, Src, and NLK in smooth muscle cells (SMC).

Figure 4. c-Kit forms a molecular complex with the regulatory proteins TAK1, Src, and NLK in smooth muscle cells (SMC). A) Diagram illustrating the proposed molecular complex between c-Kit, TAK1, Src, and NLK in SMC and their inhibitory function on NF-κB transcriptional activity. **B-C)** Co-immunoprecipitation experiments in control ($Kit^{+/+}$) and c-Kit deficient ($Kit^{W/W-v}$) SMC using anti-c-Kit **(B)** and anti-TAK1 antibodies **(C)** to pull down protein complexes. Molecular weight markers are shown on the right side of the gels, while antibodies used to detect eluted proteins are indicated on the left. IP, immunoprecipitation; IB, immunoblot.

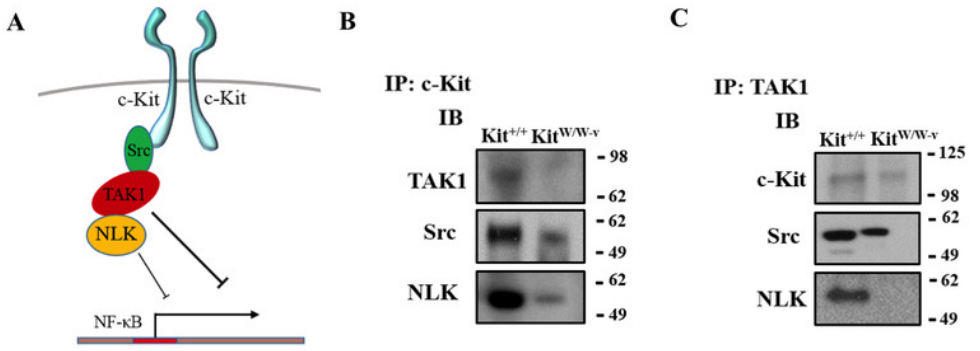

Figure 4. c-Kit forms a molecular complex with the regulatory proteins TAK1, Src, and NLK in smooth muscle cells (SMC). A) Diagram illustrating the proposed molecular complex between c-Kit, TAK1, Src, and NLK in SMC and their inhibitory function on NF-κB transcriptional activity. **B-C)** Co-immunoprecipitation experiments in control ($Kit^{+/+}$) and c-Kit deficient ($Kit^{W/W-v}$) SMC using anti-c-Kit **(B)** and anti-TAK1 antibodies **(C)** to pull down protein complexes. Molecular weight markers are shown on the right side of the gels, while antibodies used to detect eluted proteins are indicated on the left. IP, immunoprecipitation; IB, immunoblot.